Vibrationally Resolved Fluorescence from Organic Molecules near Metal Surfaces in a Scanning Tunneling Microscope

Z.-C. Dong,[1] X.-L. Guo,[1] A. S. Trifonov,[1] P. S. Dorozhkin,[1] K. Miki,[1] K. Kimura,[1] S. Yokoyama,[2] and S. Mashiko[2]

[1]*National Institute for Materials Science, 1-2-1 Sengen, Tsukuba, Ibaraki 305-0047, Japan*
[2]*Communication Research Laboratory, Kobe, Hyogo 651-2401, Japan*

Intrinsic molecular fluorescence from porphyrin molecules on Au(100) has been realized by using a nanoscale multimonolayer decoupling approach with nanoprobe excitation in the tunneling regime. The molecular origin of luminescence is established by the observed well-defined vibrationally resolved fluorescence spectra. The molecules fluoresce at low ''turn-on'' voltages for both bias polarities, suggesting an excitation mechanism via hot electron injection from either tip or substrate. The excited molecules decay radiatively through Franck-Condon π^*-π transitions.

The highly localized tunneling current of a scanning tunneling microscope (STM) can be used for excitation of light emission [1]. In contrast to detailed understanding of STM-induced luminescence (STML) on metallic [2–5] and semiconducting surfaces [6–8], the role of molecules, acting as spacers [9] or emitting fluorescence directly [10], remains controversial for molecule-covered surfaces [11–15]. Despite good optical contrasts in photon maps [9,11], no direct evidence of molecular fluorescence resulting from HOMO-LUMO (highest occupied molecular orbital–lowest unoccupied molecular orbital) radiative transitions of neutral molecules has been reported that are well justified by photoluminescence (PL) spectra. The identification of molecular fluorescence has been difficult due to its complication with plasmon-mediated emissions from substrates that are known quite tip sensitive [16]. Recently, Ho *et al.* [10] reported the first use of an oxide spacer layer for single molecule fluorescence detection. They attributed the observed fluorescence to transitions between two unoccupied molecular orbitals of anionic species. The challenging issue is the following: can intrinsic molecular fluorescence associated with HOMO-LUMO transitions be generated and detected from molecules inside a nanoenvironment such as a STM cavity? This issue is believed to be fundamentally important to the development of molecular scale electronics.

The difficulty in observing well-defined fluorescence from organic molecules near surfaces is primarily due to the quenching of molecular fluorescence when molecules are close to metal surfaces [17,18]. The realization of molecular electroluminescence on surfaces would thus depend on how effectively the emitter can be decoupled from the substrate [10]. Since energy transfer near surfaces depends dramatically on the emitter-substrate distance [17], we report here a simple approach of using molecules as both spacer and emitter, and investigate how STML evolves upon the increase of thickness. The multimonolayer stacking of selected porphyrin architecture has been found to reduce the nonradiative energy

transfer from excited molecules to metal substrates. We observe well-defined vibrationally resolved fluorescence excited by STM that matches nearly perfectly with the standard PL data of the molecule. The linewidths of spectral peaks (defined as the full width at half maximum) narrow down with increased thickness and appear to follow approximately the classical dipole theory. A quantum efficiency of $\sim 10^{-5}$ photons per tunneling electron was obtained for the molecular fluorescence at both polarities. We also observe an intriguing phenomenon of emitting photons at energies exceeding the energy of tunneling electrons. A double-barrier model is proposed to account for the occurrence of molecular fluorescence.

The experiments were performed with an ultrahigh vacuum JEOL-STM. *Meso*-tetrakis(3,5-di-tertiarybutyl-phenyl)porphyrin (H$_2$TBPP) molecules [Fig. 1(a)] were deposited onto atomically clean Au(100) substrates by sublimation from a Knudsen cell with deposition rate monitored by a microbalance and calibrated by STM images. Tungsten (W) tips were used for all experiments. STM images were taken in the constant current topographic mode with the sample biased. Photons emitted from the tunnel junction were collected by a lens system and detected by photomultiplier and spectrophotometer [12]. Luminescent spectra were acquired at room temperature over typically 10 min at a spectral resolution of 9 nm over 350–800 nm. The STML from molecules was generated in the tunneling regime at low bias (typically <3 V) and small currents (≤ 0.5 nA). The tip was positioned statically with a stable tunnel resistance, but due to thermal drift (~ 0.2 nm/min), the spectra may be averaged over several molecules.

Figure 1(b) shows how H$_2$TBPP molecules pack on Au(100) layer by layer for the molecular multimonolayer schematically shown in Fig. 1(c). The steric repulsion between phenyl and pyrrole H atoms drives the phenyl ring to rotate out of the porphyrin plane. The STM images exhibit characteristic four-lobe feature for each molecule (~ 2 nm), indicating that the porphyrin core is
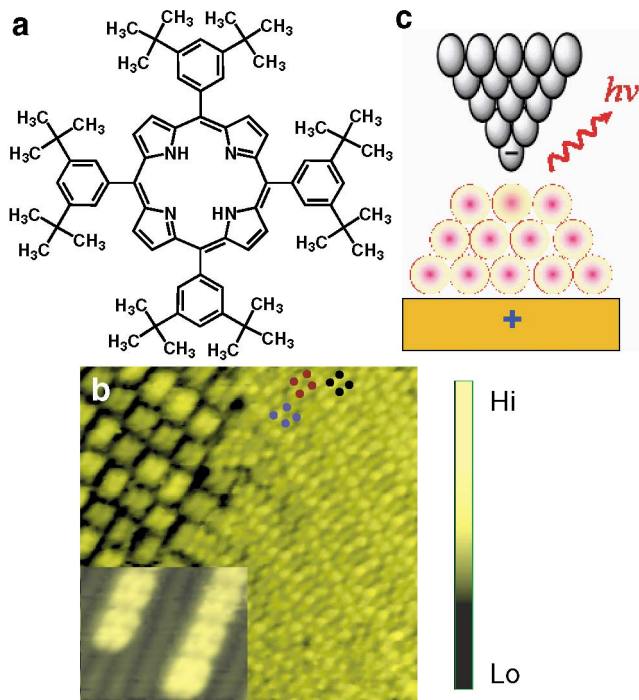
FIG. 1 (color). (a) Molecular structure of H_2TBPP. (b) STM image of molecular stacking at ~ 2.5 ML (20×20 nm^2, $+2.5$ V, 50 pA). The inset shows the adsorption conformation of the molecules on the striped Au(100) (9×8 nm^2). (c) Schematic junction geometry with multimonolayer stacking.

oriented parallel to the surface and the phenyl rings are tilted [19]. The tilt of the phenyl rings shores up the porphyrin core ~ 0.7 nm above the substrate, but the molecule-substrate interaction is still strong for the first monolayer due to hybridization between the states of molecules and substrate. The molecules are found to stack roughly in either "eclipsed"(upper-left) or "staggered" (right) manner, but STML appears essentially the same for both areas.

Optical spectroscopy is most authoritative in judging the origin of STML. The spectrum from 1 ML H_2TBPP on Au(100) shows a single-peak feature [Fig. 2(a), blue] that is characteristic of plasmon-mediated emission from the Au substrate [Fig. 2(a), brown] [2] except for the enhancement and blueshift effects [9,12]. Molecular fluorescence is quenched for one monolayer coverage, an indication of the molecule acting as a spacer to modify the STM junction geometry [9]. No direct effect of molecular orbitals was detected on the spectra, though in other cases such an effect can dominate [5]. Further electronic decoupling is required to weaken the molecule-substrate interaction for molecular fluorescence to appear [10]. Indeed, as we increase the coverage and use the bottom molecules as a spacer layer, new spectral features start to emerge. The green curve in Fig. 2(a) shows a typical spectrum at 3 ML. In addition to the plasmon-mediated band around 600 nm, a broad band at ~ 658 nm starts to emerge together with a small bump at 723 nm,
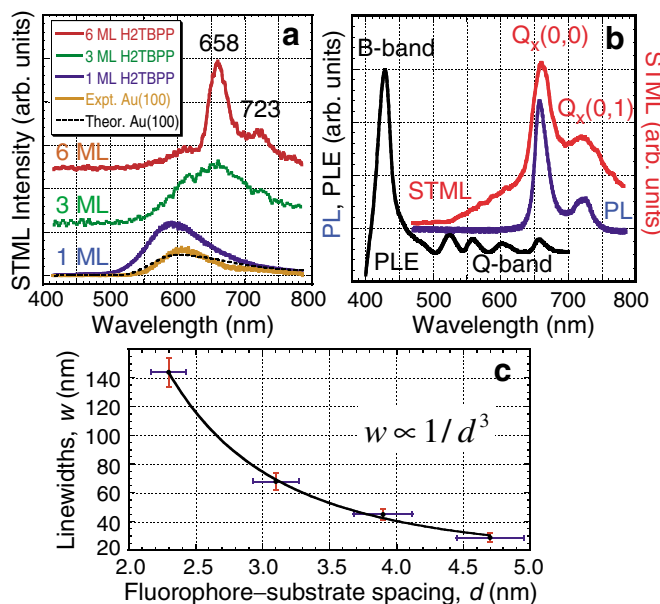

FIG. 2 (color). (a) STML spectra at $+2.8$ V and 0.5 nA for Au(100) (brown) and at different coverage of H_2TBPP (blue: 1 ML; green: 3 ML; red: 6 ML). The black curve shows theoretical simulation for Au(100) [2,12]. (b) STML spectra (red, 6 ML, $+2.8$ V, 0.2 nA) compared with PL spectra (blue) and photoluminescence excitation spectra (PLE, black). The PL spectrum was measured from a H_2TBPP thin film (~ 30 nm) using a He-Cd laser at 442 nm. (c) Distance dependence of spectral linewidths at 658 nm for STM-induced molecular fluorescence ($+2.8$ V and 0.5 nA). The four data points were for 3, 4, 5, and 6 ML. The error bars show the estimated standard deviations for the linewidth (vertically) and spacing (horizontally).

suggesting luminescence contributions from molecules. These two additional peaks become sharper with increased coverage while the plasmon-mediated band is suppressed [Fig. 2(a), red, 6 ML].

The molecular origin of the STM-induced emission bands at 658 and 723 nm [Fig. 2(b), red] is clearly established upon comparison with the PL spectrum of H_2TBPP [Fig. 2(b), blue]. The matching of two sharp peaks is nearly perfect, which also suggests the same decay channel of excited states despite different excitation mechanisms. The luminescence of porphyrins originates from π^*-π transitions with nearly degenerate $a_{1u}(\pi)$ and $a_{2u}(\pi)$ MOs as HOMO and degenerate $e_g(\pi^*)$ MO as LUMO (D_{4h} is assumed for simplicity) [20]. The peak at 658 nm can be assigned to the $Q_x(0,0)$ fluorescence while the 723-nm peak to the vibronic overtone $Q_x(0,1)$ [20]. Such assignment is further supported by (i) the coincidence between the $Q_x(0,0)$ absorption and fluorescence transitions and (ii) the same peak spacing of 0.16 eV for the Q-band vibronic structure in both fluorescence and excitation spectra [Fig. 2(b), black]. Such vibrational mode is also confirmed by the infrared spectrum with absorption at 1290 cm^{-1}, and usually pertains to the $C_{pyrrole}$-phenyl vibration [21,22].

The linewidths of spectral peaks at 658 nm, obtained via fitting to a Lorentzian line shape, narrow down as the molecules stack up layer by layer [Fig. 2(c)], suggesting the dominance of the fluorescence from the top-layer molecules. With increased thickness, the emitter-substrate coupling is weakened, which results in decreased lifetime-broadening and narrowed linewidths (w). Since the molecules stack on top of each other with porphyrin cores horizontally oriented, the height of each monolayer is viewed approximately the same. The luminescent core-substrate spacing (d) is estimated based on the first layer spacing of ~0.7 nm and the molecular height of ~0.8 nm. A power-law fit to the w-d plot yields an approximate $w \propto 1/d^n$ with $n = 2.8(5)$, which is close to the $1/d^3$ dependency and thus suggests a dipole-dipole energy transfer in nature from molecular excited states to the bulk substrate [18]. The classical dipole theory [17] appears still valid for distances less than 5 nm.

As expected for molecular fluorescence, the peak positions at 658 and 723 nm remain constant for different excitation voltages [Fig. 3(a)], because the radiative decay is associated with the HOMO-LUMO gap of the molecule. The increase in intensity at higher bias arises from the increased number of vibronic states available for electron tunneling [10]. Of particular interest is the oc-

FIG. 3 (color). Bias dependency of STML at 6 ML and 0.5 nA. (a) Fluorescence spectra at different voltages, showing constant peak positions and "forbidden" transitions. (b) "bipolar" molecular fluorescence (± 2.5 V). (c) quantum efficiency of fluorescence as a function of bias.

currence of molecular fluorescence at excitation voltages (e.g., $+1.8$ V) less than the energy of photons emitted (peaked at 1.9 eV). Such "energy forbidden" transitions were previously observed in organic light emitting diodes [23]. It is also noteworthy that H_2TBPP molecules fluoresce at both polarities [Fig. 3(b)]. The emission intensity at positive bias is higher than that at negative bias. Such trend is further confirmed by the bias dependency of emission intensities in Fig. 3(c) where most of the surface plasmon contribution other than the tail was filtered out by using a sharp highpass cutoff filter (620 nm). Two low "turn-on" voltages were observed, $+1.5$ V for positive bias and -1.7 V for negative bias. The drop in intensity above $+3.5$ and -3.0 V is probably due to damage of molecules at high bias.

The bipolar operation with comparable intensities suggests that (i) the energy levels of emitting molecules are not pinned to the substrate but shifted with applied bias and (ii) the coupling for the tip-molecule-substrate is not very asymmetric despite the dissimilar tip-molecule-substrate structure [24]. The latter implies that the voltage drop for the molecular multimonolayer is comparable to that between the tip and molecule. The barrier heights for carrier injection and related onset voltages depend on how molecular energy levels are aligned with respect to the Fermi levels of electrodes [25]. When HOMO and LUMO states fall inside the energy window defined by the electrochemical potentials of the tip and substrate, electrons can be injected into the LUMO and holes into the HOMO [24]. Molecular fluorescence at bias above 1.9 eV is relatively easy to understand since 1.9 eV is the optical band gap of H_2TBPP molecules [the onset of optical absorption in Fig. 2(b)] although the HOMO-LUMO gap includes additional exciton binding energy [25]. However, for energy forbidden transitions, the mechanism of its occurrence is still not clear and awaits further experimental and theoretical studies. Possible causes may pertain to thermally assisted tunneling injection of holes via energetically distributed hole traps above HOMO [25,26] or energy level shifts due to charging of molecules [24]. The two-electron excitation mechanism proposed for Na overlayers on Cu(111) [27] is probably unlikely in the present case because the "forbidden" transitions were observed at very low currents.

The generation of STM-induced molecular fluorescence from H_2TBPP appears related to its hole-transport character typical of aromatic-amine compounds [26,28]. STM-induced molecular fluorescence was not observed for a similar multimonolayer of electron-transport tris-(8-hydroxyquinoline) aluminium molecules. The STM probably plays a role in injecting efficiently minority electron carriers into the unoccupied orbitals of H_2TBPP at both polarities. The relatively higher intensity at positive bias with respect to the negative suggests that the HOMO is relatively closer to the Fermi level of electrodes [24], in agreement with the hole-transport
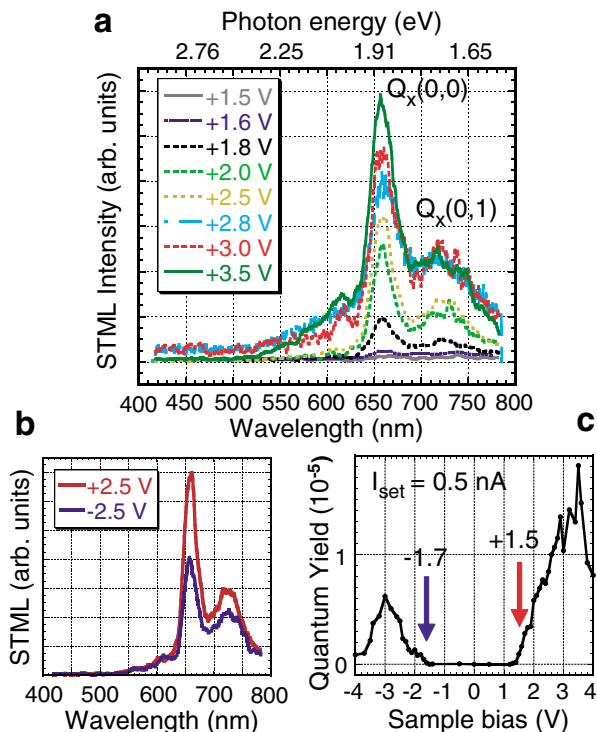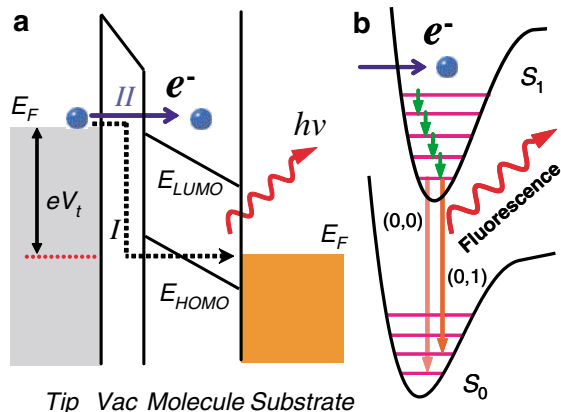
FIG. 4 (color online). (a) Schematic diagram showing two concurrent STML mechanisms for molecular multimonolayer on metal substrates. Process I: plasmon-mediated emission via inelastic tunneling; Process II: molecular fluorescence via hot electron injection. (b) Molecular fluorescence via Frank-Condon transitions from excited state to ground state.

character of the molecule by analogy with the band picture for a p-type semiconductor.

On the basis of the occurrence of molecular fluorescence at low bias and suppression of plasmon-mediated emission at increased thickness, the mechanism of STML from a molecular multimonolayer is proposed in Fig. 4(a). The plasmon-mediated emission at ~ 600 nm and the molecular fluorescence at 658 and 723 nm arise from two simultaneous but substantially different decay mechanisms [4,10]. Process I refers to the inelastic tunneling excitation events that lead to plasmon-mediated emissions associated with the substrate. Such an excitation effect is suppressed dramatically at increased thickness because direct tunneling from the tip to the metal substrate becomes less likely.

Molecular fluorescence is generated by the hot electron injection excitation followed by the radiative decay associated with the HOMO-LUMO transitions (Process II). Once bias voltages are above the electron injection barrier, electrons tunnel elastically through the vacuum barrier into unoccupied molecular orbitals while the HOMO is partially emptied simultaneously. Nevertheless, as shown in Fig. 4(b), no matter where the electrons are injected into the electronically excited vibronic states, the excited states will first go through fast radiationless decay to the ground vibrational level of the lowest π^* state. Then, a radiative decay follows through Franck-Condon transitions to the electronic ground state, giving rise to the vibronic $Q_x(0,0)$ and $Q_x(0,1)$ fluorescence.

The mechanism proposed in Fig. 4(a) is essentially a double-barrier model with a vacuum barrier on the W tip side and a Schottkylike barrier at the molecule-gold interface. When substrates are negatively biased, electrons from the gold substrate have to tunnel through the Schottkylike barrier to create electronically excited states of molecules.

In summary, clear STM-induced molecular fluorescence from organic molecules on metal surfaces has been realized via multimonolayer decoupling. The vibrationally resolved molecular fluorescence is found to originate from the HOMO-LUMO radiative transitions of neutral molecules via Franck-Condon principles.

[1] J. H. Coombs et al., J. Microsc. **152**, 325 (1988).
[2] R. Berndt, J. K. Gimzewski, and P. Johansson, Phys. Rev. Lett. **67**, 3796 (1991).
[3] Y. Uehara, T. Fujita, and S. Ushioda, Phys. Rev. Lett. **83**, 2445 (1999).
[4] G. Hoffmann, J. Kliewer, and R. Berndt, Phys. Rev. Lett. **87**, 176803 (2001).
[5] G. V. Nazin, X. H. Qiu, and W. Ho, Phys. Rev. Lett. **90**, 216110 (2003).
[6] D. L. Abraham et al., Appl. Phys. Lett. **56**, 1564 (1990).
[7] A. Downes and M. E. Welland, Phys. Rev. Lett. **81**, 1857 (1998).
[8] C. Thirstrup et al., Phys. Rev. Lett. **82**, 1241 (1999).
[9] G. Hoffmann, L. Libioulle, and R. Berndt, Phys. Rev. B **65**, 212107 (2002).
[10] X. H. Qiu, G. V. Nazin, and W. Ho, Science **299**, 542 (2003).
[11] R. Berndt et al., Science **262**, 1425 (1993).
[12] Z.-C. Dong et al., Surf. Sci. **532−535**, 237 (2003).
[13] S. F. Alvarado, L. Libioulle, and P. F. Seidler, Synth. Met. **91**, 69 (1997).
[14] K. Sakamoto et al., Surf. Sci. **502−503**, 149 (2002).
[15] F. Touhari et al., Appl. Phys. Lett. **79**, 527 (2001).
[16] J. Aizpurua, S. P. Apell, and R. Berndt, Phys. Rev. B **62**, 2065 (2000).
[17] R. R. Chance, A. Prock, and R. Silbey, Adv. Chem. Phys. **37**, 1 (1978).
[18] W. L. Barnes, J. Mod. Opt. **45**, 661 (1998).
[19] T. A. Jung, R. R. Schlittler, and J. K. Gimzewski, Nature (London) **386**, 696 (1997).
[20] M. Gouterman, in *The Porphyrins*, edited by D. Dolphin (Academic Press, New York, 1978), Vol. 3, Chap. 1, pp. 1–165.
[21] R. A. Reed et al., J. Phys. Chem. **95**, 9720 (1991).
[22] S. F. Alvarado et al., Phys. Rev. B **56**, 1269 (1997). The authors reported luminescent spectra from polymers ~ 200 nm thick and under field emissions (100 V).
[23] Y. G. Ma et al., Appl. Phys. Lett. **74**, 1361 (1999).
[24] J. Buker and G. Kirczenow, Phys. Rev. B **66**, 245306 (2002).
[25] J. C. Scott, J. Vac. Sci. Technol. A **21**, 521 (2003).
[26] T. J. Savenije and A. Goossens, Phys. Rev. B **64**, 115323 (2001).
[27] G. Hoffmann, R. Berndt, and P. Johansson, Phys. Rev. Lett. **90**, 046803 (2003).
[28] M. Stolka, J. F. Yanus, and D. M. Pai, J. Phys. Chem. **88**, 4707 (1984).